Chapter 6

Solar Resource Variability

Richard Perez
Atmospheric Sciences Research Center, University at Albany

Thomas E. Hoff
Clean Power Research

Chapter Outline

6.1. Introduction 133
6.2. Quantifying Solar-Resource Variability 135
6.3. The Dispersion-Smoothing Effect 136
6.4. The General Case of an Arbitrarily Dispersed Fleet of Solar Generators 142
6.5. Variability Impact on the Distribution and Transmission System 143
6.6. A Final Note on the Smoothing Effect 146
References 146

6.1. INTRODUCTION

In this chapter, we focus on the short-term temporal variability of the solar resource caused by weather and passing clouds, corresponding to timescales of seconds to tens of minutes. This type of variability is illustrated in Figure 6.1.

Variability is primarily caused by (1) the movement of the Sun and (2) the movement and evolution of clouds. Variability due to the movement of the Sun is precisely predictable, while that due to the movement of clouds is not. The predictable component is the result of solar geometry—the Sun's apparent motion in the sky induces changes in the resource. These changes are not noticeable for very short time intervals (seconds to minutes), but become influential for longer time intervals, particularly near sunrise and sunset. This chapter focuses on the less predictable part of variability: the "noise" caused by the motion and evolution of cloud fields.

Short-term variability is relevant to the operation of solar-power systems and their impact on the power grids to which they are connected: A small cloud

Solar Energy Forecasting and Resource Assessment. ISBN: 9780123971777

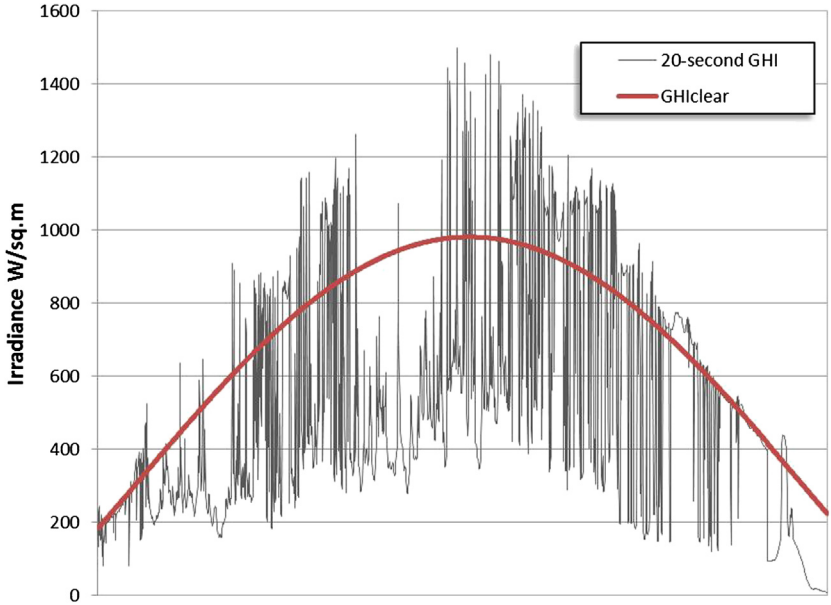

FIGURE 6.1 Global irradiance (GHI) and clear-sky global irradiance (GHI_{clear}) sampled at 20 s on a high-variability day. *(Data from the Oklahoma ARM Extended Facility Network.) This figure is reproduced in color in the color section.*

passing in front of the Sun can cause a small PV installation to go from full production to almost none and then back to full production in a matter of seconds—this impact is of concern to grid operators. There is a perception that solar-generation variability as illustrated in Figure 6.1 could pose major problems for utility distribution and transmission networks. The work of Skartveit and Olseth (1992) on understanding and parameterizing short-term variability was long one of the few references on this topic until increasing PV penetration, initially in Europe, raised the level of interest in solar energy variability (Wiemken et al. 2001, Woyte et al. 2007). The topic has generated a considerable amount of new research during the last few years (e.g., Frank et al. 2011; Hinkelman et al. 2011; Hoff and Perez 2010, 2012; Hoff, 2011; Jamaly et al. 2012; Kankiewicz et al. 2011; Kuszamaul et al. 2010; Lave and Kleissl 2010, 2013; Lave et al. 2011, 2012; Mills and Wiser 2010; Mills et al. 2009; Murata et al. 2009; Norris and Hoff 2011; Perez and Hoff 2011; Perez et al 2011a, 2011b; Perez and Fthenakis 2012; Sengupta 2011; Stein et al. 2011).

The term *ramp rate* is often used to characterize solar variability. It originated in the utility industry to describe power plants coming online and going offline in response to demand (ramping up or down). It has been widely used by the wind industry to describe the sudden and noncontrollable coming online or going offline of a large number of units as a result of local changes in wind speed such as those associated with passing weather fronts. The analogy with

wind-power ramp rates may be appropriate for longer timescales at the upper range of the domain considered in this chapter, whereby regional output may ramp up or down from the effect of weather fronts over an hour or more. The term *fluctuation*, however, may be a more appropriate term to describe the short-term variability illustrated in Figure 6.1 that occurs over seconds to minutes.

6.2. QUANTIFYING SOLAR-RESOURCE VARIABILITY

Properly quantifying variability requires definitions of (1) the physical quantity that varies, (2) the time interval over which this quantity varies, and (3) the period during which variability is considered.

The *physical quantity* of power output (P) of a solar system or an ensemble, or *fleet*, of solar systems is of the highest interest to energy producers and grid operators. P is a function of solar-generator specifications and the solar resource. A general measure of the solar resource for nonconcentrating flat-plate[1] solar-system configurations is global horizontal irradiance (GHI). Short-term GHI variability includes the effect of predictable factors due to changes in Sun position and unpredictable factors due to weather/clouds. The effect of unpredictable factors is captured by the clear-sky index (Kt^*), defined as the ratio of GHI to $\text{GHI}_{\text{clear}}$.[2] Thus, Kt^* is the key parameter of interest since GHI is inferred from the clear-sky index and Sun position, and P is inferred from GHI.

Time interval is the time (Δt) over which the change in the selected physical quantity, $\Delta Kt^*_{\Delta t}$, is considered. It can range from a few seconds to hours depending on the particular concern of the user. As will be shown, the relevant time interval is directly related to the geographical footprint of the considered solar resource and hence to its impact on the power grid from a transformer on a distribution feeder to a regional control area.

Time period is the number of time intervals over which variability is defined; that is, it is a multiple of Δt.

Variability metric for single location is defined here as the standard deviation of the change in power output. This variability is directly proportional to the change in the clear-sky index across all locations using the specified time interval ($\Delta Kt^*_{\Delta t}$) over the selected time period (Hoff and Perez 2010). That is, (power output) variability is directly proportional to

$$\sigma\left(\Delta Kt^*_{\Delta t}\right) = \sqrt{VAR\left[\Delta Kt^*_{\Delta t}\right]} \tag{6.1}$$

1. Direct normal rradiance (DNI) would be the relevant quantity if concentrating technologies were considered.

2. The range of the global index is reduced as the Sun's elevation decreases, because the relative weight of diffuse irradiance increases during clear-sky conditions.

6.3. THE DISPERSION-SMOOTHING EFFECT

It has long been observed that the combined (relative) variability of multiple solar generators (or wind generators) is less than the variability experienced by a single system (e.g., Wiemken et al. 2001, Murata et al. 2009). For instance, Figure 6.2 compares the variability of 1 location to that of 25 locations within a 4 × 4 km footprint.

Uncorrelated locations represent a smoothing effect that can be precisely quantified when the fluctuations experienced by different locations are comparable and uncorrelated (Mills and Wiser 2010, Hoff and Perez 2010). In this case, the variability of an ensemble of identical systems in independent locations, σ_{fleet}, is given by

$$\sigma_{\text{fleet}} = \frac{1}{\sqrt{N}}\sigma_i \tag{6.2}$$

where σ_i is the variability experienced by a single location, and N is the number of locations. This is a direct result of the strong law of large numbers that states that the average of a sequence of independent random variables having a common distribution will, with probability 1, converge to the mean of that distribution as the number of observations goes to infinity (Ross 1988, 346).

With *partially correlated locations,* we know intuitively (1) that if two systems are located right beside each other, they will fluctuate almost in sync and the resulting variability will be nearly equal, in relative terms, to the variability of each individual location; and (2) that if two systems are located far away from each other, they will fluctuate independently of each other and a smoothing effect following (equation 6.2) will occur.

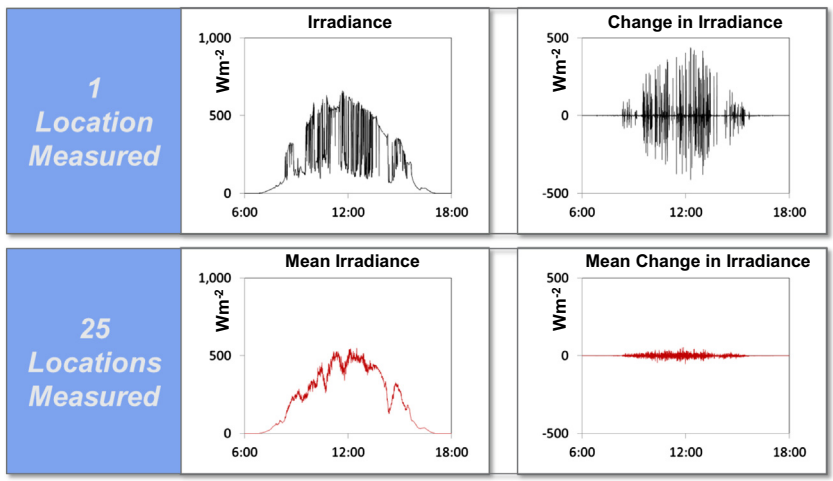

FIGURE 6.2 Dispersion-smoothing effect occurring at 25 locations dispersed over a 4 × 4 km area *(Data from the Cordelia Junction network, San Francisco Bay area, California.) This figure is reproduced in color in the color section.*

For cases that lie between these two extremes, smoothing will occur but to a lesser degree than the $1/\sqrt{N}$ trend:

$$\sigma_{\text{pair}} = \frac{\sqrt{\rho + 1}}{\sqrt{2}} \sigma_i \tag{6.3}$$

where the site-pair correlation ρ ranges between 0 and 1. Therefore,

- It is important to determine how site-pair correlation varies as a function of the factors that influence it. These factors include (1) the distance between the stations (D), (2) the considered time interval (Δt), and (3) the speed (CS) of the clouds producing the fluctuations. The impact of distance is understandable per the above discussion: Correlation is equal to 1 for collocated sites and gradually decreases to 0 until the sites are distant enough so as to fluctuate independently.
- The time interval (Δt) that defines the considered fluctuation is relevant because it relates to the size of the cloud perturbations causing the fluctuation. High-frequency fluctuations are caused by the fine structure of cloud fields (e.g., small individual clouds). The correlation of these fluctuations rapidly decreases with distance. Lower-frequency fluctuations are caused by larger-scale structures, such as entire cloud fields or weather fronts. Two stations that are uncorrelated at the small-structure level may experience almost the same synchronized variability at a longer timescale and thus be highly correlated at that scale.
- Cloud speed is relevant because it is the major underlying cause of variability: Simply stated, clouds that do not move do not cause fluctuations. Assuming for the sake of argument that moving cloud structures remain largely unchanged over the considered time period, the faster the structure travels, (1) the smaller the time shift in the signal between two stations and the larger the correlation between them (for cloud size greater than sensor

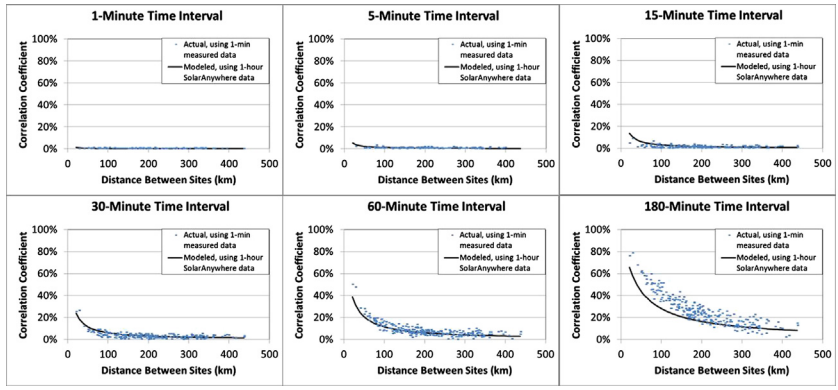

FIGURE 6.3 Site-pair correlation as a function of distance (D) and time interval (Δt) for stations in the ARM network. *(From Mills and Wiser 2009.) This figure is reproduced in color in the color section.*

spacing); and (2) the longer the distance at which two sites along the direction of cloud speed experience the same fluctuations for a given time interval and thus the longer the distance at which they exhibit a given correlation.

Note that for a given cloud size, cloud speed defines the relevant fluctuation time interval.

The relationship between σ_{pair}, Δt, *CS*, and *D* has been studied using several sources of empirical evidence. For example, Mills and Wiser (2010) analyzed data from the ARM network (Stokes and Schwartz 1994), including 32 stations measuring GHI at a 20 s rate. They noted the exponential decay of σ_{pair} as a function of station distance and observed that the rate of exponential decay is a continuous function of the considered time interval Δt. However, the shortest distance between any two stations in the ARM network being 20 km, they were not able to observe trends for Δt below 10 min. (See Figure 6.3.)

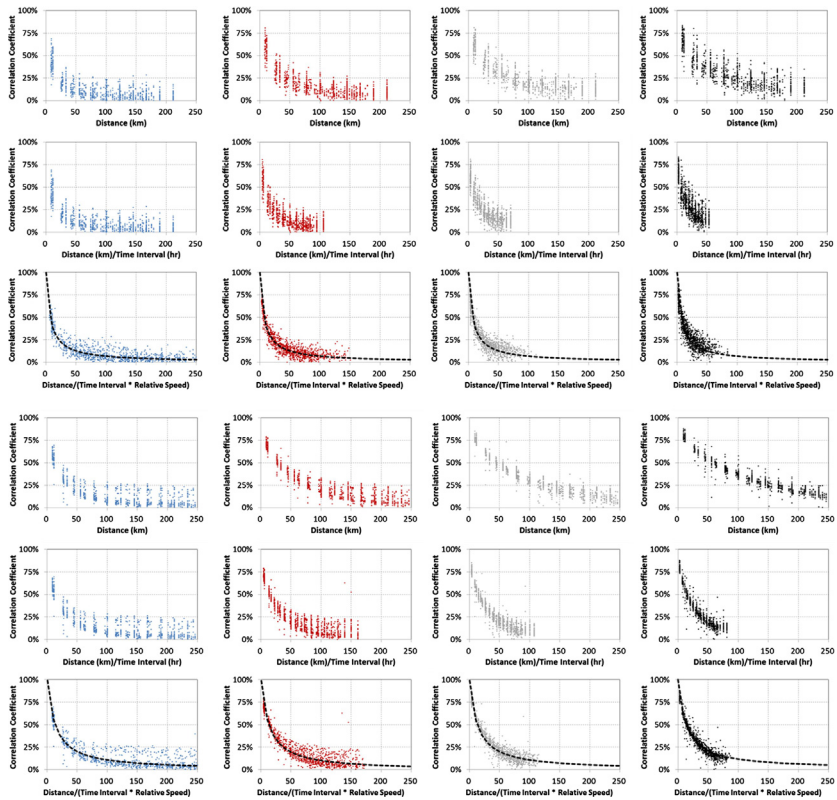

FIGURE 6.4 Site-pair variability correlation as a function of distance derived from hourly 10 km–resolution satellite data for California (*top*) and the Great Plains (*bottom*). The top row in each case represents ρ as a function of distance. The bottom row expresses this relationship as a function of the ratio between *D* and $\Delta t \times$ implied *CS*, showing that the distance relationship is predictably dependent on Δt and *CS*. *This figure is reproduced in color in the color section.*

Hoff and Perez (2012) repeated this exercise using standard-resolution (10 km) hourly satellite-derived irradiances. They observed a similar exponential decay and a predictable dependence on Δt for time intervals of 1, 2, and 3 h. They also noted that the exponential decay was different for the different regions they analyzed and attributed these differences to prevailing regional cloud speeds. (See Figure 6.4.)

Perez et al. (2012) analyzed the 20 s ARM data and added one-dimensional virtual networks around each ARM station using satellite-derived cloud speeds to project irradiance downwind from each station and assuming conservation of cloud structures. By doing so, they were able to analyze data with high frequency ($\Delta t = 20$ s) and short distances. They quantified the correlation decay with distance and Δt, and defined a no-correlation threshold as the point beyond which two stations' fluctuations become uncorrelated. They observed that this distance is linearly related to the considered Δt. They cautioned that their results would have to be confirmed by analyzing real two-dimensional, high-density network data—in particular, the negative correlation peaks that are apparent in Figure 6.4 are a result of the negative correlation occurring downwind as cloud structures pass, unchanged, from the real to the virtual location; these negative peaks should be only partially apparent in the case of two-dimensional networks.

Hoff & Norris. (2010) analyzed data from a modular network composed of 25 stations with a total footprint ranging from 400 m × 400 m to 4 km × 4 km (Figure 6.5). They observed the same trend as in virtual one-dimensional networks, including the negative correlation in the direction of cloud speed. They qualitatively observed that cloud speed, acquired independently from satellite cloud motion, affects the rate of decay.

Perez et al. (2011a) used (true two-dimensional) high-resolution (1 km, 1 min) satellite-derived data to systematically quantify the ρ_{pair} distance trends

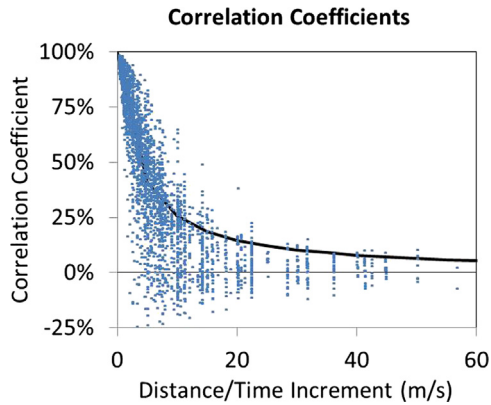

FIGURE 6.5 Site-pair correlation as a function of distance for time intervals ranging from 10 s to 5 min in Cordelia Junction, California. Data are extracted from a 25-station 400 m × 400 m network. Note that some of the site pairs (likely oriented in the direction of cloud motion) exhibit the negative correlation peak noted in the virtual networks. *This figure is reproduced in color in the color section.*

as a function of Δt and CS for several regions in the United States (Figure 6.6), and proposed the following empirical formulation relating σ_{pair}, Δt, CS, and D:

$$\rho_{\text{pair}} = e^{Ln\ (0.2)D/1.5\ \Delta t\ CS} \tag{6.4}$$

The linear relationship between the no-correlation threshold distance and the considered time interval noted by Perez et al. (2012) was confirmed, but was

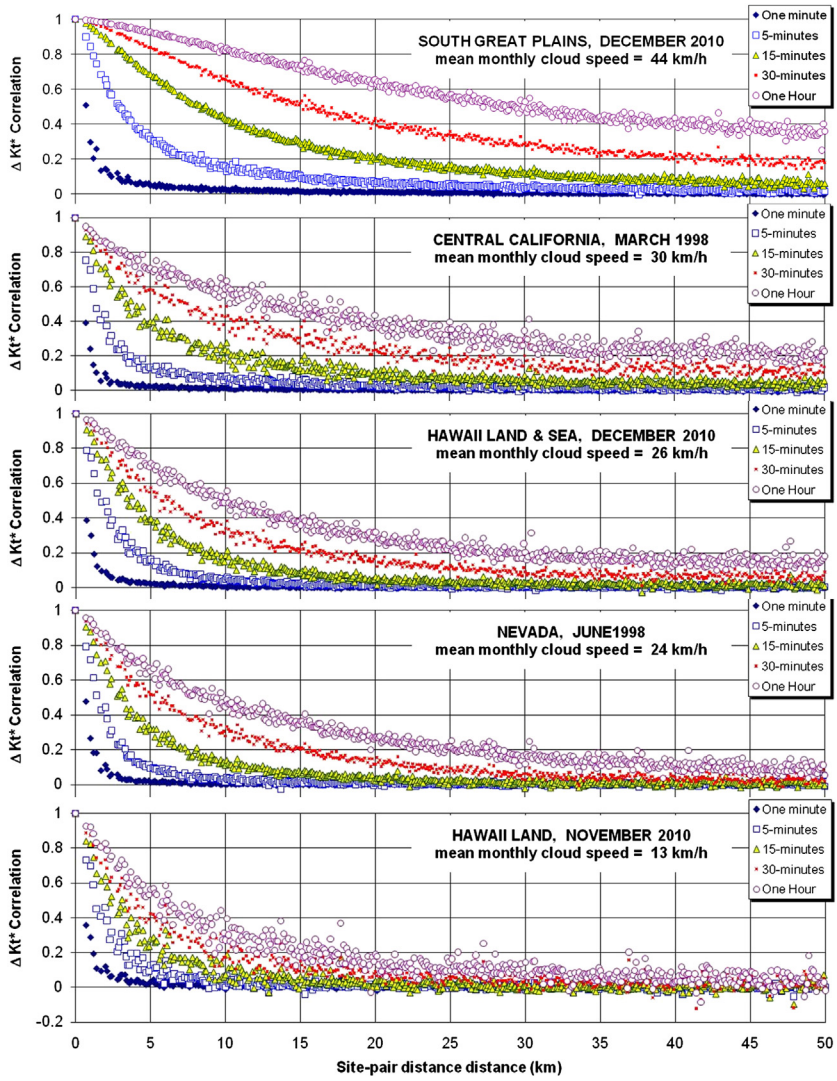

FIGURE 6.6 Site-pair correlation observed with 1min 1 km resolution satellite-derived irradiances in several U.S. regions and illustrating the respective effect of Δt, D, and CS. *This figure is reproduced in color in the color section.*

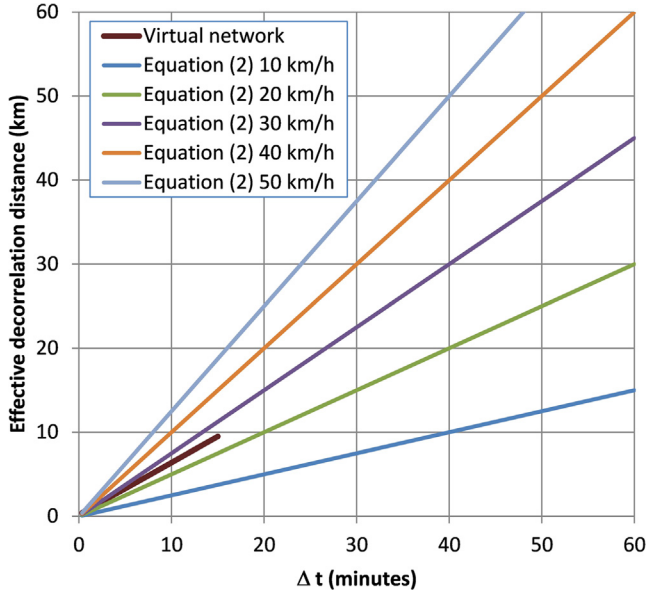

FIGURE 6.7 Applying equation 6.4 to estimate the effective site-pair decorrelation distance as a function of Δt and *CS*. The short line labeled "Virtual network" represents the preliminary estimate of this relationship based on limited evidence. *This figure is reproduced in color in the color section.*

adjusted to reflect the dependence of this relationship upon cloud speed. This is shown in Figure 6.7.

Bing et al. (2012) analyzed 30 highly variable days from a newly deployed 66-station network distributed over the Sacramento Municipal Utility District's (SMUD's) territory and covering an area of roughly 200 km^2. Each station measures irradiance at a time rate of 1 min. Cloud speeds aloft were obtained from satellite imagery. The researchers' results confirmed the preliminary empirical relationship linking ρ_{pair}, Δt, *CS*, and *D* (Figure 6.8).

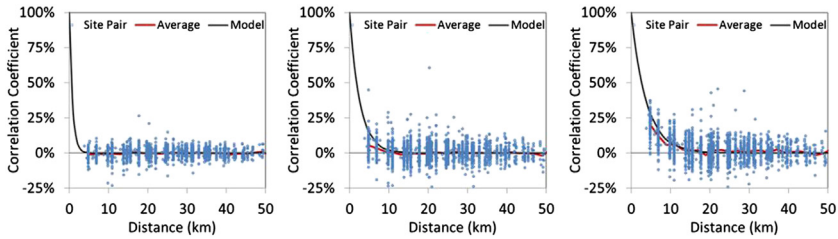

FIGURE 6.8 Site-pair variability correlation vs. distance for three fluctuation timescales using data from the SMUD 66-station network. The solid line represents the mean of a model (equation 6.4)based on Δt, *D*, and *CS*. *This figure is reproduced in color in the color section.*

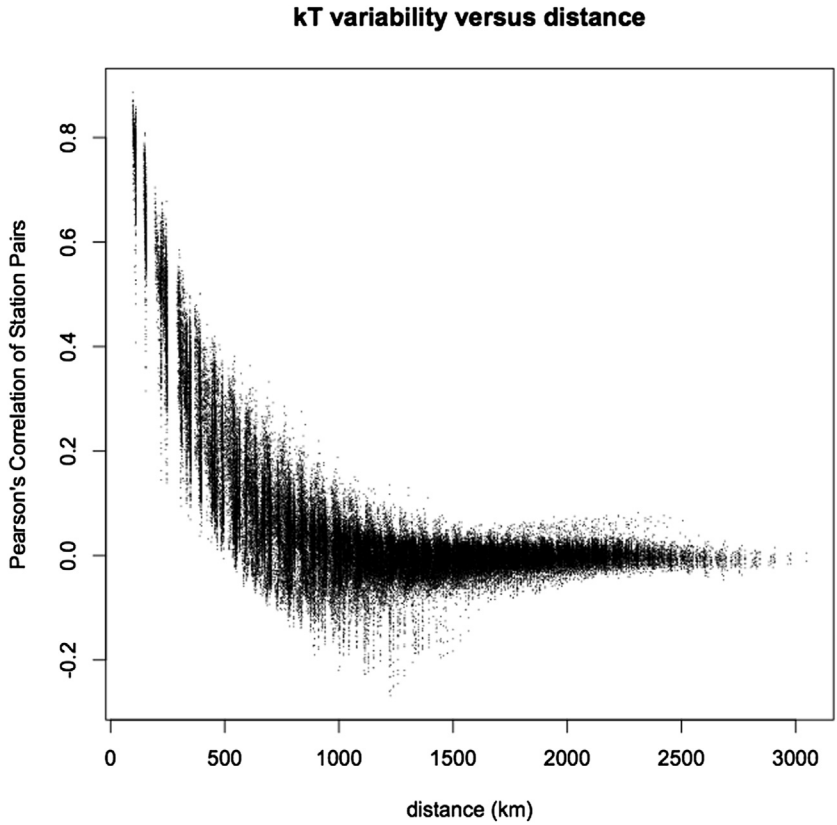

FIGURE 6.9 Site-pair variability correlation as a function of distance for $\Delta t = 24$ h obtained using daily total irradiances from NASA/SSE (2012). *(From Perez and Fthenakis 2012)*

Interestingly, there is evidence that the trend outlined in Figure 6.7 for Δts ranging from a few seconds to a few hours is conserved for much longer time intervals of days, as noted by Perez et al. (2012; Figure 6.9).

6.4. THE GENERAL CASE OF AN ARBITRARILY DISPERSED FLEET OF SOLAR GENERATORS

We discussed the ideal case of N identical uncorrelated systems with identical variability σ_i, resulting in a relative fleet variability equal to $1/\sqrt{N}$ that of individual installations. We also showed how this relationship is modified when correlation is not equal to 0 and how correlation evolves as a function of distance, time interval, and prevailing cloud speed.

General situations where dispersion smoothing occurs fall into two broad categories of centralized and dispersed solar (PV) generation. The centralized case may be approximated to a series of identical point systems regularly

spaced at known distances. A more general situation is the case of dispersed generation that involves nonidentical systems distributed at arbitrary distances and hence experiencing varying degrees of site-pair correlation.

Because systems are not always identical, the output of the fleet, and thus its variability, may be influenced by the size of its individual systems—and the variability of each system, which may itself be the result of spatial intra-array smoothing in the case of large arrays. It is thus necessary to return to an absolute formulation of variability based on the power output of each system, $\sigma^i(\Delta P^i_{\Delta t})$, where i represents the ith system in the fleet.

The variability of the fleet—that is, the standard deviation of change in fleet output, $\sigma^{\text{fleet}}_{\Delta t}$, —equals the square root of the variance of the sum of the changes in output from each of the individual systems. The variance of the sum, however, equals the sum of the covariance of all possible combinations.

$$\sigma^{\text{fleet}}_{\Delta t} = \sqrt{\text{VAR}\left[\sum_{n=1}^{N} \Delta P^n_{\Delta t}\right]} = \sqrt{\sum_{i=1}^{N}\sum_{j=1}^{N} \text{COV}\left(\Delta P^i_{\Delta t}, \Delta P^j_{\Delta t}\right)} \quad (6.5)$$

The covariance between any two plants equals the standard deviations of each of the locations times the correlation coefficient between the two locations (i.e., $\text{COV}(\Delta P^i_{\Delta t}, \Delta P^j_{\Delta t}) = \sigma^i_{\Delta t}\, \sigma^j_{\Delta t}\, \rho^{i,j}_{\Delta t}$). As a result,

$$\sigma^{\text{fleet}}_{\Delta t} = \sqrt{\sum_{i=1}^{N}\sum_{j=1}^{N} \sigma^i_{\Delta t}\, \sigma^j_{\Delta t}\, \rho^{i,j}_{\Delta t}} \quad (6.6)$$

The critical observation to be made about equation (6.6) is that the standard deviation of changes in fleet output is based entirely on the standard deviation of changes in plant output at each location and the correlation between the locations, which can be gauged from empirical formulations such as proposed in equation 6.4.

6.5. VARIABILITY IMPACT ON THE DISTRIBUTION AND TRANSMISSION SYSTEM

Although some of the evidence presented in this chapter is empirical (i.e., based on imperfect measurements over a limited time spans and covering a limited climatic range), it overwhelmingly suggests that (1) solar-resource variability is a predictable function of the considered timescales and geographic scales and of the velocity of the variability-causing cloud structures; and (2) the variability of any solar-generation configuration, from a single small system to a fleet of systems that are arbitrarily spaced and sized, including geographically extended individual solar farms, can be adequately estimated.

In particular, it can be stated with a fair degree of certainty that 20 s fluctuations should not be an issue for solar-power plants distributed over more than 500 m (even for cloud speeds equal to 50 km/h). Figure 6.10 shows an example for the city of New York, comparing measured variability on a highly variable day from a single point to a city-wide distributed-generation network.

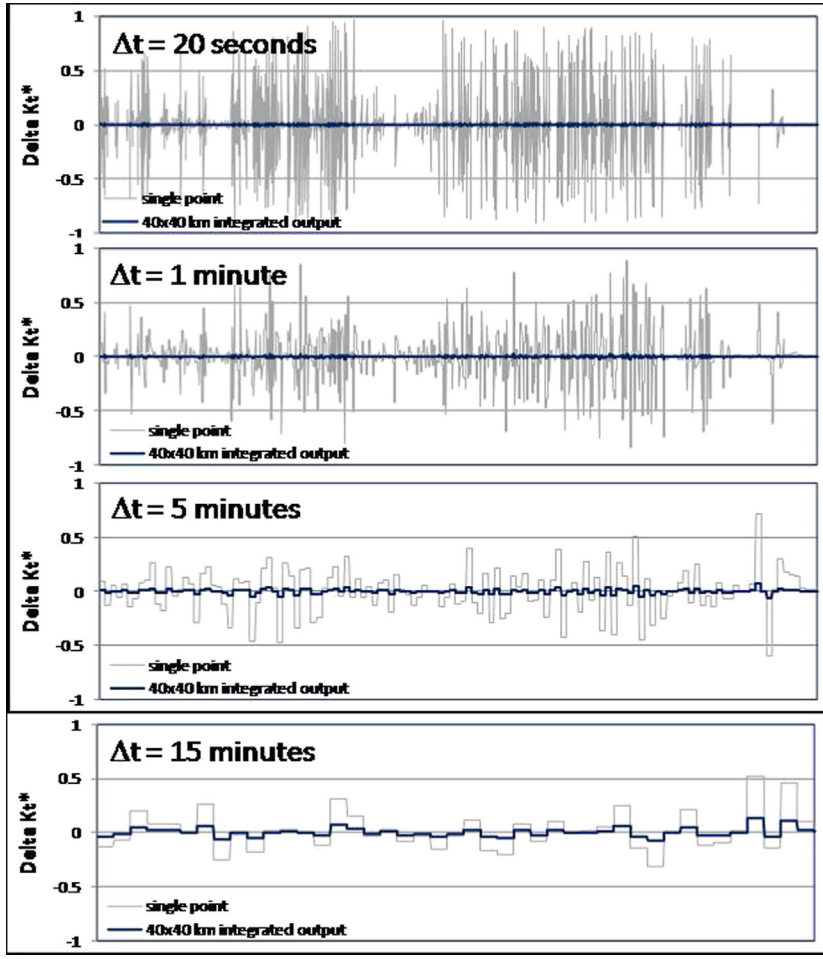

FIGURE 6.10 Smoothing effect at the scale of a metropolitan area comparing single-site and modeled 40 km × 40 km extended fluctuations for different timescales. *This figure is reproduced in color in the color section.*

Figure 6.11 illustrates the implications of the temporal and spatial characteristics of variability for utility integration.

Short-term fluctuations and ramp rates of less than 20 s will affect small individual systems, but should be minimized when a fleet of such systems covers an area of a few square kilometers. At the system level, these fluctuations can (rarely) cause localized voltage disturbances and can cause systems to trip offline. The best way to address them is at the interconnection-hardware level, which can include appropriate "shock absorbers" to increase their electrical inertia and eliminate such risks. An analogy is a car that is designed to operate perfectly on a rough road if it has the proper suspension without having to anticipate and account for every bump.

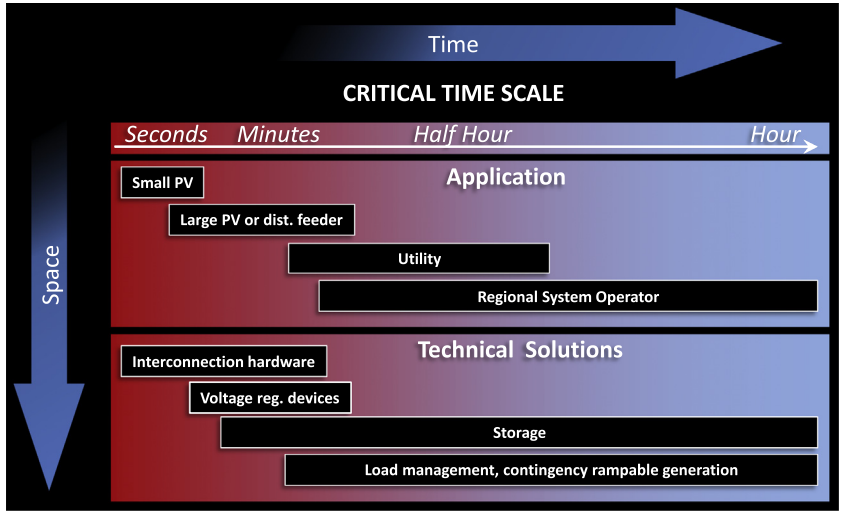

FIGURE 6.11 Temporal and spatial fluctuation scales of relevance to PV-grid interconnection issues and technical solutions, from a single installation on a small feeder to dispersed generation within a utility balancing area. *This figure is reproduced in color in the color section.*

Fluctuations of the order of a few minutes remain a concern for areas of a few square kilometers,which are representative of a fleet of distributed systems served by a substation or a very large centralized power plant (several hundreds of megawatts). However, in the case of the distributed fleet, these fluctuations should be of minimal concern for utility-wide generation. Mitigation at this level involves both the interconnection shock absorbers mentioned above and some level of voltage and power regulation, including short-term storage of a few minutes in the case of large centralized arrays, injecting vast amounts of power on the grid so as to "buy time" for the ramping up and down of associated combined cycle gas turbines that can now accommodate ramp-up times approaching 5 min. Forecasting the exact timing of such variability will become valuable at the upper range of this temporal-geographical scale, especially if the area is a separate grid (such as on an island). Here again the car analogy is short inclines where the driver must actively participate and modulate power input to maintain speed.

Fluctuations of a half-hour to an hour and longer may have implications for the utility system and will require load-following action, in terms of reserve (or, worst-case, contingency) generation, load management, and storage. Fortunately, the temporal and spatial scales involved (over a half hour and many tens of kilometers) and the accuracy of solar-radiation (forecast) resources available at these scales make the management of these fluctuations possible and effective. At the upper range of this scale, regional balancing areas serving several regional utilities should be concerned only with fluctuations of more than one hour.

In practice, a utility or developer can use the results presented in this chapter in conjunction with historical solar-resource satellite-derived data to estimate the variability of any proposed PV configuration—centralized or dispersed—with a footprint of 1 km or more. Equation 6.4 provides guidance for selecting the Δt of concern for the considered footprint (the smaller the footprint, the higher the required frequency). Since satellite-derived irradiance models are now capable of producing data at frequencies approaching 1/min and 1 km resolution, the variability of any footprint in excess of 1 km can be inferred directly from satellite-data time series. In addition, Hoff (2011) has proposed and patented a methodology to infer variability on any temporal or spatial scale starting from a known reference point (e.g., 1km/1min), thus extending the use of satellite data down to a single system where the relevant time interval may be of the order of seconds.

6.6. A FINAL NOTE ON THE SMOOTHING EFFECT

It is helpful at this point to make a final comment on the force behind the smoothing effect, given that it is seen so consistently across a broad set of research results. The relationship that links the spatial and temporal scales of cloud-induced fluctuations appears to be connected to the long observed fractal nature of cloud fields (Mandelbrot 1982) that are self-similar at all scales. In other words, a fine cloud structure causing fluctuations of the order of seconds is self-similar to a much larger structure. This larger structure will cause similar fluctuations but at larger temporal and spatial scales as long as cloud speed does not change between the two. Interestingly, these space-time characteristics have equivalences in other aspects of solar-resource assessment: It is well known, for instance, that the dispersion accuracy of both satellite remote-sensing and forecast models (MAE or RMSE) improves as the geographical extent of the considered solar resource increases from a single point to a region (Hoff and Perez 2012, Lorenz et al. 2011). Similarly, it has recently been shown that the peak shaving-capacity credit of a dispersed solar resource increases and the loss-of-load probability decreases as the dispersion of the solar resource increases (Perez and Hoff 2012).

REFERENCES

Bing, J., Krishnani, P., Bartholomy, O., Hoff, T., Perez, R., 2012. Solar Monitoring, Forecasting, and Variability Assessment at SMUD. Proc. World Renewable Energy Forum, Denver, CO.

Frank, J., Freedman, J., Brower, M., Schnitzer, M., 2011. Development of High Frequency Solar Data. Proc. Solar 2011, American Solar Energy Society Conf., Raleigh, NC.

Gueymard, C., Wilcox, S., 2011. Assessment of spatial and temporal variability in the US solar resource from radiometric measurements and predictions from models using ground-based or satellite data. Solar Energy 85 (5), 1068–1084.

Hinkelman, L., George, R., Sengupta, M., 2011. Differences between Along-Wind and Cross-Wind Solar Variability. Proc. Solar 2011, American Solar Energy Society Conf., Raleigh, NC.

Hoff, T. E. (2011). U.S. Patent Applications: Computer-Implemented System and Method for Determining Point-to-Point Correlation of Sky Clearness for Photovoltaic Power Generation Fleet Output Estimation (Application Number 13/190,435); Computer-Implemented System and Method for Estimating Power Data for a Photovoltaic Power Generation Fleet (Application Number 13/190,442); Computer-Implemented System and Method for Efficiently Performing Area-to-Point Conversion of Satellite Imagery for Photovoltaic Power Generation Fleet Output Estimation(Application Number 13/190,449).

Hoff, T.E., Perez, R., 2010. Quantifying PV power Output Variability. Solar Energy 84 (2010), 1782–1793.

Hoff, T.E., Perez, R., 2012. Modeling PV Fleet Output Variability. Solar Energy 86 (8), 2177–2189.

Hoff, T.E., Perez, R., 2012b. Predicting Short-Term Variability of High-Penetration PV. Proc. World Renewable Energy Forum, Denver, CO.

Hoff, T.E., Norris, B., 2010. Mobile High-Density Irradiance Sensor Network: Cordelia Junction Personal Communication.

Jamaly, S., Bosch, J., Kleissl, J., 2012. Aggregate Ramp Rates of Distributed Photovoltaic Systems in San Diego County. IEEE Transactions on Sustainable Energy. in press.

Kankiewicz, A., Sengupta, M., Li, J., 2011. Cloud Meteorology and Utility Scale variability. Proc. Solar 2011, American Solar Energy Society Conf., Raleigh, NC.

Kuszamaul, S., Ellis, A., Stein, J., Johnson, L., 2010. Lanai High-Density Irradiance Sensor Network for Characterizing Solar Resource Variability of MW-Scale PV System. 35th Photovoltaic Specialists Conference, Honolulu. June, 2010.

Lave, M., Kleissl, J., Stein, J., 2012. A Wavelet-based Variability Model (WVM) for Solar PV Powerplants. IEEE Transactions on Sustainable Energy 99, 1–9.

Lave, M., Kleissl, J., 2010. Solar Intermittency of Four Sites Across the State of Colorado. Renewable Energy 35, 2867–2873.

Lave, M., Kleissl, J., 2013. Cloud speed impact on solar variability scaling – Application to the wavelet variability model. Solar Energy 91, 11–21.

Lave, M., Kleissl, J., Arias-Castro, E., 2011. High-frequency fluctuations in clear-sky index. Solar Energy 86 (8), 2190–2199.

Lorenz, E., Scheidsteger, T., Hurka, J., Heinemann, D., Kurz, C., 2011. Regional PV power prediction for improved grid integration. Progress in Photovoltaics 19 (7), 757–771.

Mandelbrot, B., 1982. The fractal Geometry of Nature. WH Freeman and Co, New York, 1982.

Mills, A., Alstrom, M., Brower, M., Ellis, A., George, R., Hoff, T., Kroposki, B., Lenox, C., Miller, N., Stein, J., Wan, Y., 2009. Understanding variability and uncertainty of photovoltaics for integration with the electric power system. Lawrence Berkeley National Laboratory Technical Report LBNL-2855E.

Mills, A., Wiser, R., 2010. Implications of Wide-Area Geographic Diversity for Short-Term Variability of Solar Power. Lawrence Berkeley National Laboratory Technical Report LBNL-3884E.

Murata, A., Yamaguchi, H., Otani, K., 2009. A Method of Estimating the Output Fluctuation of Many Photovoltaic Power Generation Systems Dispersed in a Wide Area. Electrical Engineering in Japan 166 (4), 9–19.

NASA/SSE, 2012. Surface meteorology and Solar Energy. http://eosweb.larc.nasa.gov/sse/.

Norris, B.L., Hoff, T.E., 2011. Determining Storage Reserves for Regulating Solar Variability. Electrical Energy Storage Applications and Technologies Biennial International Conference, San Diego, 2011.

Perez, M., Fthenakis, V., 2012. Quantifying Long Time Scale Solar Resource Variability. Proc. World Renewable Energy Forum, Denver, CO.

Perez, R., Hoff, T., 2012b. Dispersed PV Generation Solar Resource Variability. George Washington Solar Institute 2012 Symposium. GW University, Washington, DC.

Perez, R., Hoff, T.E., 2011. Solar Resource Variability: Myth and Fact. Solar Today. August/September 2011.

Perez, R., Kivalov, S., Schlemmer, J., Hemker Jr., C., Hoff, T.E., 2011b. Parameterization of site-specific short-term irradiance variability. Solar Energy 85 (2011), 1343–1353.

Perez, R., Kivalov, S., Schlemmer, J., Hemker Jr., C., Hoff, T.E., 2012. "Short-term irradiance variability correlation as a function of distance." Solar Energy 86 (8), 2170–2176.

Perez, R., Hoff, T., Kivalov, S., 2011a. Spatial and temporal characteristics of solar radiation variability. Proc. of International Solar Energy (ISES) World Congress, Kassel, Germany.

Ross, S., 1988. A First Course in Probability. Macmillan Publishing Company.

Sengupta, M., 2011. Measurement and Modeling of Solar and PV Output Variability. Proc. Solar 2011. American Solar Energy Society Conf., Raleigh, NC.

Skartveit, A., Olseth, J.A., 1992. The Probability Density of Autocorrelation of Short-term Global and beam irradiance. Solar Energy 46 (9), 477–488.

Stein, J., Ellis, A., Hansen, C., Chadliev, V., 2011. Simulation of 1-Minute Power Output from Utility-Scale Photovoltaic generation Systems. Proc. Solar 2011. American Solar Energy Society Conf., Raleigh, NC.

Stokes, G.M., Schwartz, S.E., 1994. The atmospheric radiation measurement (ARM) program: programmatic background and design of the cloud and radiation test bed. Bulletin of American Meteorological Society 75, 1201–1221.

Vignola, F., 2001. Variability of Solar Radiation over Short Time Intervals. Proc. Solar 2001, American Solar Energy Society Conf., Washington, D.C.

Wiemken, E., Beyer, H.G., Heydenreich, W., Kiefer, K., 2001. Power Characteristics of PV ensembles: Experience from the combined power productivity of 100 grid-connected systems distributed over Germany. Solar Energy 70, 513–519.

Woyte, A., Belmans, R., Nijs, J., 2007. Fluctuations in instantaneous clearness index: Analysis and statistics. Solar Energy 81 (2), 195–206.